ATTENUATION OF GAMMA RADIATION BY URANIUM

by

Robert Anthony Meisenheimer

A Thesis Submitted to the
Graduate Faculty in Partial Fulfillment of
The Requirements for the Degree of
MASTER OF SCIENCE

Major Subject: Nuclear Engineering

Approved:

Iowa State University
Of Science and Technology
Ames, Iowa

1960

TABLE OF CONTENTS

I. INTRODUCTION

Shortly after the discovery of X-rays and, a few years later, of radiation from radioactive substances, it became apparent that there were possible harmful effects of these radiations. Ever since that moment shielding against penetrating radiation has been a matter of concern and study.

With the advent of nuclear chain reactors this problem of radiation shielding was magnified greatly. No longer was science dealing with the relatively low source strengths of radioactive materials but now the intensities of available radioactive sources were increased by many powers of ten. Naturally this requires correspondingly larger and more effective shields.

This increased importance of shielding has been responsible for extensive study of gamma radiation attenuation during the past decade. The attenuation of gamma radiation is of prime importance because of its characteristic nature. All types of radiation are present in the nuclear reactor but the charged particles, by virtue of their electric charge, interact strongly with the atomic electrons of the matter they pass through and very quickly lose their energy. Thus it is the neutrons and gamma rays that provide the main burden of the shielding problem. Gamma radiation was selected for this study primarily due to the greater degree of freedom in pro-

cedure, equipment, and source material.

Experimental determination, as is often the case, lagged behind theoretical calculations during the initial phases of study concerning the problem. However improved counting techniques since 1947 have shifted the emphasis and it is now possible to obtain accurate experimental results. The greater percentage of experimental data taken today is obtained by using a collimated beam of monoenergetic gamma rays and calculating the absorption coefficients of the absorbing material with regard to the total amount of electromagnetic radiation penetrating the material. Because of the various interaction processes, the penetrating radiation from the absorber covers the entire energy range from the energy of the initial gamma ray through the X-ray region.

This variation of the energy spectrum of gamma radiation with increased absorber thickness is of added importance since the variation is not constant over the energy range. By use of gamma ray scintillation crystals, photo multiplier tubes, and recording spectrometers, an accurate gamma ray energy spectrum can be obtained.

A collimated beam of gamma radiation is utilized in this investigation so as to provide better means of correlating this data with present theory and previous experimental results most of which are based on narrow beam collimation. In

this investigation uranium is the absorbing material. Uranium was selected because as a heavy element, it should be a highly efficient gamma shield. Also contributing to its selection is the pressing need to find an economical role in the nuclear industry for the large quantities of depleted uranium which are becoming increasingly available but, as yet, fill no need.

If by using this arrangement, the variations in the energy spectrum can be correlated with existing theory, the accuracy of the experimental method of determining gamma radiation would be verified.

II. LITERATURE REVIEW AND DISCUSSION OF THEORY

It is beyond the purpose of this study to present an extended description of the various processes by which gamma rays interact with matter. The subject is treated in detail in a number of standard references and the present discussion is only an outline to give a suitable background for the investigation. Among the numerous references on the fundamentals of gamma ray interaction processes are a large number of papers, reports, and books. The latter include Segre (11), Friedlander and Kennedy (4), and Kaplan (8); all of whom present a rather straightforward approach. Other useful presentations have been given by Fano (3), White (13), Bethe and Ashkin (1), Snyder and Powell (12), and Davisson (2). Although somewhat more difficult, the classic reference for a basic understanding of the fundamental phenomena is the treatise by Heitler (7). Two more recent reports by Goldstein and Wilkins (6), and Goldstein (5) each contain an excellent presentation on gamma ray attenuation covering all aspects of the problem and including considerable data.

A. The Interactions of Gamma Rays with Matter

Even upon restricting the energy range to the region of interest from 20 kew to 10 Mev, there are a large number of mechanisms by which photons can interact with matter. Table 1

lists these interactions in rough order of importance for attenuation calculation.

Table.1. Gamma ray interaction processes

A. Primary	
	1. Photoelectric effect
	2. Compton scattering
	3. Pair production
B. Secondary	
	4. Coherent (Rayleigh) Electron scattering
	5. Annihilation radiation
	6. Fluorescence radiation
	7. Bremsstrahlung
	8. Thomson scattering from the nucleus
	9. Delbruck or Potential scattering
	10. Multiple Bragg scattering
	11. Nuclear interactions
	a. photoeffects
	b. scattering
	12. Radiative corrections to lower order processes

1. Photoelectric effect

In the photoelectric effect an incident photon transfers all of its energy to one of the atomic electrons, ejecting it from the atom. The energy of this emitted electron is equal to the incident photon energy less the ionization energy of the electron. Hence this process can occur only when the energy of the photon is greater than the binding energy of the electron. However for photon energies very large compared to the ionization energy, the photoelectric effect becomes relatively unimportant. Since the binding energy increases rapidly as Z increases, the photoelectric effect becomes more prominent for heavy elements and the photoelectric cross-section increases. Heitler (7) states that this cross section is proportional to Z^5 while Goldstein (5) considers that it is between Z^4 and Z^5. Thus for the heavier elements, the photoelectric effect predominates. In fact for uranium, it provides one-half the total absorption coefficient up to .620 Mev as indicated by Goldstein (5).

2. Compton scattering

Whereas by the preceeding interaction or absorptive process the photon disappeared entirely, the Compton effect, by contrast, is a scattering process which alters the direction and energy of the incident photons but does not destroy it. Herein lies the major difficulty in calculating gamma ray at-

tenuation.

As the Compton effect is the scattering of photons by free or loosely bound electrons, these electrons being essentially free, are without interaction among themselves, and the effect is strictly additive. Thus the characteristics can be developed for a single electron and the cross sections multiplied by Z to obtain the atomic cross section. Extensive compilations have been performed on this phenomena, the best of which probably are by Latter and Kahn (9), and Nelms (10).

Kaplan (8) presents the standard treatment of Compton scattering and covers the main features quite well. This approach gives the energy of a scattered photon in terms of the initial energy and the scattering angle by

$$h\nu = \frac{h\nu_o}{1 + \frac{h\nu_o}{m_o c^2}(1 - \cos\theta)} \qquad 1$$

or in terms of the electron rest mass energy,

$$E = \frac{E_o}{1 + E_o(1 - \cos\theta)} \qquad 2$$

The discussion so far refers only to a single Compton scattering process. Thus in order to treat the contribution of Compton scattering, it is necessary to calculate the probability that such a scattering process will occur. This was

developed on the basis of relativistic quantum mechanics by Klein and Nishina and is covered quite thoroughly by Heitler (7). The Klein Nishina formula for the total scattering cross section per electron is

$$e\sigma_c(E) = \frac{3}{4}\phi_o \left\{\frac{1+E_o}{E_o^2}\left[\frac{2(1+E_o)}{1+2E_o} - \frac{1}{E_o}\ln(1+2E_o)\right] + \frac{1}{2E_o}\ln(1+2E_o) - \frac{1+3E_o}{(1+2E_o)^2}\right\}, \qquad 3$$

where E_o is in electron rest mass units and ϕ_o is given by

$$\phi_o = \frac{8\pi}{3}\left(\frac{e^2}{m_o c^2}\right)^2 = 6.65 \times 10^{-25}\text{cm}^2.$$

Besides the total cross section, it is also necessary to know the differential cross section in angle, i.e., the cross section for scattering by a given angle. This is given by the Klein Nishina formula:

$$\sigma(\theta)\, d\Omega = \frac{3}{16\pi}\frac{E^2}{E_o^2}\left(\frac{E_o}{E} + \frac{E}{E_o} - \sin^2\theta\right) d\Omega. \qquad 4$$

In the preceeding discussion it was shown that the cross section per atom varied as Z and now from these equations, it can be shown that the total scattering cross section is dependent on the photon energies. Data given by Goldstein (5) illustrate that over the major portion of this energy region, the Compton

effect is the predominate interaction. Even for an element as heavy as uranium, the Compton effect forms the major part of the total absorption coefficient from 0.6 to 5.0 Mev.

3. Pair production

In pair production all the energy of the incident photon is transformed into the creation of an electron pair--an elec tron and a position. The total kinetic energy is equal to the energy of the photon minus the rest mass of the pair or twice the rest mass of an electron. Therefore pair production has a threshold energy of $2 M_0C^2$ or 1.022 Mev below which it cannot take place. Goldstein (5) gives a good account of this process and illustrates the increasing effect of Z on the amount of pair production.

As the energy range of this investigation is below the threshold energy, further discussion of this process is deemed unnecessary.

4. Secondary interaction processes

The various secondary processes listed in Table 1 are only of minute importance. This is particularly so in the energy range of this investigation where the overwhelming majority of photon interactions are through one of the proc- esses listed above. As the actual calculations of gamma ray

attenuation consider only those previously mentioned, the remainder will be neglected in this investigation. Both Goldstein (5) and Goldstein and Wilkins (6) offer rather comprehensive discussions of these processes.

B. Gamma Ray Absorption Coefficients

If a beam of incident photons of flux density I_o passes through an absorber of thickness x, then the intensity I_x transmitted through that thickness is given by

$$I_x = I_o e^{-\mu x} \quad . \qquad 5$$

This exponential attenuation formula is the well known Lambert's law of absorption. Its derivation is relatively simple and is arrived at by considering that the number of collisions made in path length d_x by photons passing in unit time through unit cross sectional area of the beam is $I\sigma ndx$, where σ is the collision cross section and n the number of atoms per unit volume. By substituting the absorption coefficient μ, equal to $n\sigma$, this value becomes $I\,\mu dx$. If these collisions are purely absorptive, this number of collisions must be exactly equal to the decrease in the flux density I over the distance dx

$$-dI = I\,\mu dx \qquad 6$$

Of course the solution to this equation is Lambert's law given previously by equation 5.

From the considerations of the preceeding section it is clear that the total photon cross section to be used in attenuation calculations is given by the sum of the cross sections for photoelectric effect, Compton scattering, and pair production:

$$\sigma = \sigma_{pe} + \sigma_{c} + \sigma_{pp} \qquad 7$$

This total cross section is usually described as the mass absorption coefficient, μ, and expressed in cm^2/gm. Numerous tables of absorption coefficients are in existence, based in varying proportions on calculations and measurements in narrow beam geometry. Probably the most important of these are those by Snyder and Powell (12), Latter and Kahn (9), and G. R. White (13). The latter is the most recent and is believed to contain values accurate to within 2 per cent.

C. Methods of Calculating Gamma Ray Attenuation

To specify a photon beam, it must be known how many photons are going in what direction with what energy at what point in space. This information is given by a flux density function of position, energy, and direction, $N(\vec{r}, E, \vec{\Omega})$. This function is so defined that $N(\vec{r}, E, \vec{\Omega})dEd\Omega$ gives the number of photons at $\vec{r}$, with energy E in range dE, going in the direction

specified by the unit vector $\vec{\Omega}$, within the element of solid angle $d\Omega$, which cross in unit time a unit differential element of area whose normal is in the direction $\vec{\Omega}$. The term N is usually called the angular number flux. Corresponding to N is the angular energy flux, $I(\vec{r},E,\vec{\Omega})$ which refers to the energy of the photons rather than to their number. These are related by $I = EN$.

After rather extensive calculations, which are thoroughly described in both Goldstein (5), and Goldstein and Wilkins (6), the Boltzmann transport equation is developed:

$$\nabla\cdot\vec{\Omega}\, I+\mu I = \iint I(\vec{r},E',\vec{\Omega}')n\sigma\,(\vec{\Omega}'\rightarrow\vec{\Omega},\ E'\rightarrow E)\,\frac{E\,dE'}{E'}\,d\Omega' + S(\vec{r},E,\vec{\Omega}), \qquad 8$$

where $\sigma(\vec{\Omega}'\rightarrow\vec{\Omega},\ E'\rightarrow E)$ is the differential cross section for scattering from the direction $\vec{\Omega}'$ to $\vec{\Omega}$ and from the energy E' to E, per unit solid angle and energy range, and S refers to the energy source function.

To this date, no one has yet found a method of solution to the transport equation without involving very intensive and complicated computations. In fact only three such methods have been successfully developed. These are the method of successive scatterings, the method of moments, and the method of random sampling or more commonly called the Monte Carlo

technique. These methods are quite adequately described in Goldstein (5). Goldstein and Wilkins (6) have applied the method of moments to their study and achieved quite excellent results which are very thoroughly listed in this report.

III. EQUIPMENT

The equipment used in this investigation and the experimental arrangement are shown in Figure 1. Figure 2 shows the source as it is mounted and the varying thicknesses of uranium absorbers. A more detailed description follows.

A. Source

The source used in this experiment was cesium-barium 137. This isotope pair emits a gamma ray with an energy of 0.662 Mev due to the decay schemes

$$Cs^{137} \xrightarrow{33y} Ba^{137m} + 0.52 \text{ Mev } \beta$$

and

$$Ba^{137m} \xrightarrow{2.6m} Ba^{137} + 0.662 \text{ Mev } \gamma.$$

The source consisted of a cesium chloride solution evaporated into a small inset in a circular plexiglass disk, one inch in diameter and one half inch thick. The plexiglass was in turn mounted on a plywood stand. The strength of the source was 0.5 millicuries ± 5 per cent and due to the long half life involved it remained essentially constant over the period of experimental work.

B. Absorbers

Uranium was the absorbing material. It was prepared by Mr. Everett Taylor of the Ames Laboratory in the form of cir-

Figure 1. Experimental equipment
A. Probe in lead shield
B. Lead collimating bricks with uranium absorber in place
C. Source
D. Spectrometer
E. Scaler

Figure 2. Mounted source and uranium absorbers

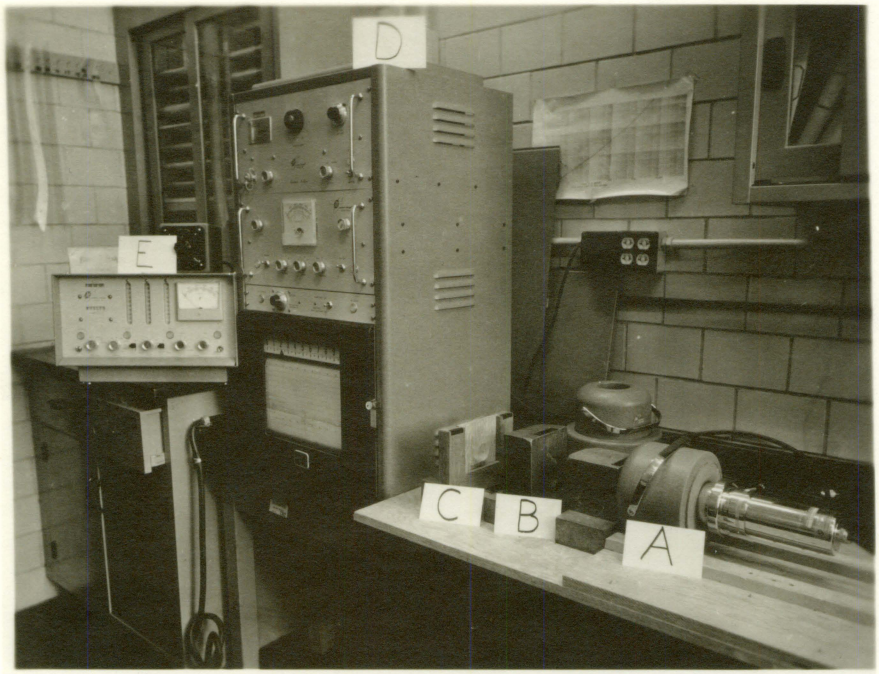
D
E
C
B
A

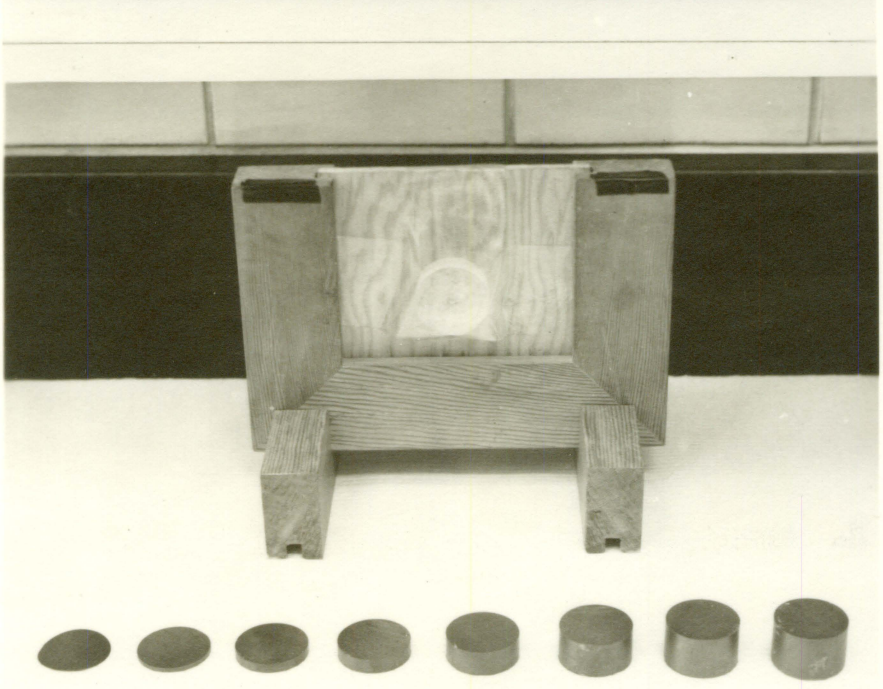

cular disks cut from a five inch long uranium bar with a diameter of 1.370 inches. Eight separate absorber thicknesses were used with thickness ranging from 0.033 inches to 0.921 inches as shown in Table 2. The absorber in use was held in place over the hole in the lead brick adjacent to the source on the side away from the source.

Table 2. Absorber thicknesses

Sample	Thickness (inches)	Weight (grams)	Cross sectional area (cm^2)	Thickness (gm/cm^2)
1	0.033	12.7096	9.5	1.338
2	0.102	46.4266	9.5	4.887
3	0.199	90.8294	9.5	9.561
4	0.303	138.6720	9.5	14.597
5	0.504	230.08	9.5	24.22
6	0.704	321.6	9.5	33.85
7	0.840	384.0	9.5	40.42
8	0.921	420.2	9.5	44.23

An aluminum absorber of 1.269 gm/cm^2 thickness was placed over the near hole in the lead brick adjacent to the uranium absorber for the purpose of eliminating the beta radiation.

C. Detector

The detector used in the experimental work was a Nuclear-Chicago Model DS 5 Scintillation Counter. This includes a

basic probe, a crystal adapter, and the scintillation crystal. The basic probe is made up of the housing, inner lead shielding, RCA-6655 photo multiplier tube, preamplifier circuit, and attached cables.

The scintillation crystal was a one inch diameter by one inch high thalium activated sodium iodide crystal hermetically sealed in a 1/32 inch aluminum can.

D. Spectrometer

The scintillation detector was connected to a Nuclear-Chicago Model 1820 Recording Spectrometer. This is a single channel differential pulse-height analyzer which automatically scans the pulse height spectrum and graphically records the input pulse rate versus pulse height on a paper strip chart. It includes a radiation analyzer, a count rate meter, and a recorder.

The pulses from the scintillation detector are fed into a linear amplifier in the radiation analyzer and then into both of two amplitude discriminating circuits. The base level discriminator sets the voltage level below which all pulses are rejected. The base level can be adjusted from 1 to 100 volts by the base level control. From the known pulse height of a source, the base level can be calibrated by means of a high voltage control. The upper discriminator is referenced

to the base level discriminator. A voltage of from 0 to 10 volts above base level voltage can be set by means of the window width control. Both of these discriminators feed into an anticoincidence circuit which rejects pulses received simultaneously from both discriminators and passes only those pulses received alone from the base level discriminator. For operation as a recording spectrometer, scanning of the radiation energy range is produced by a linear sweep of the base level discriminator voltage. This is accomplished by motor driving the base level control at a standard rate of one-half hour per complete scan.

The selected pulses from the radiation analyzer are fed into the count rate unit which provides a controllable amount of integration. The output signal, which is proportional to the number of pulses per minute, is fed to the visual meter and also to the chart recorder.

The recorder is used to obtain a large linear presentation of the radiation spectrograms. The input signal is fed into a self balancing d-c potentiometer which drives the recording pen. The count rate is then indicated by pen displacement, and the radiation energy is represented by the distance along the time axis of the chart.

E. Scaler

A Nuclear-Chicago Model 181 A Scaler was used to accurately calibrate the base level voltage.

IV. PROCEDURE

The equipment was arranged on a table as shown in Figure 1. The table was placed in the center of the room to minimize scattering from the walls. At least one hour warm-up time was allowed for each experimental run. The spectrometer would then be calibrated with the C_s-B_a^{137} source, the base level set at 662 kev, and a window width of 2 volts by adjusting the high voltage until the maximum count rate was obtained on the scaler. During all experimental work the spectrometer was set with a gain of 4:1 and a time constant of ten seconds. Since there was considerable variation in the resultant count rate due to the large absorber thicknesses used and the strong source, the count range varied from 10,000 to 300 counts per minute depending on the absorber in use.

With the spectrometer fully calibrated and adjusted, the base level control was set at 0.800 Mev. With a uranium absorber in position the chart and base level drive were turned on. The spectrometer was calibrated before and after each run and the results were discarded if it was found that the peak pulse height had shifted during that run.

The data were obtained in the form of radiation spectrograms for varying absorber thicknesses. These data were also compiled in tabular form as shown in Appendix A. The sweep

of the base level drive was cut off at a lower limit of 0.100 Mev. This was necessitated by the extremely high count rates encountered below this setting due to the characteristic uranium and the barium K X-ray peaks.

V. RESULTS AND DISCUSSION

A. General Characteristics of the Spectrograms

A representative group of the spectrograms obtained in this investigation are shown in Figures 3 through 6 in order of increasing absorber thickness. Data for these and all other spectrograms are given in Appendix A. The changes in the rate and energy of the penetrating radiation with increasing absorber thickness are graphically illustrated in these figures. Because of the radiative nature of the absorber itself, spectrograms were also obtained with the absorber in place and source removed. Thus in this manner an accurate recording of the entire background contribution could be gained. These spectrograms were all quite similar and as could be expected, the only variation was the increased rate in proportion to the increasing absorber thickness. Because of this high degree of similarity only two of these spectrograms are shown. These are Figures 3 and 6 and are for the thinnest and thickest uranium absorbers respectively. Note that these two plates are superimposed on the original spectrogram for the total radiation from the source and for that particular absorber. These are shown in this manner to more clearly illustrate the relative contribution from the gamma ray source compared to the uranium absorber background. The third curve on Figure 6 is a plot of the difference between

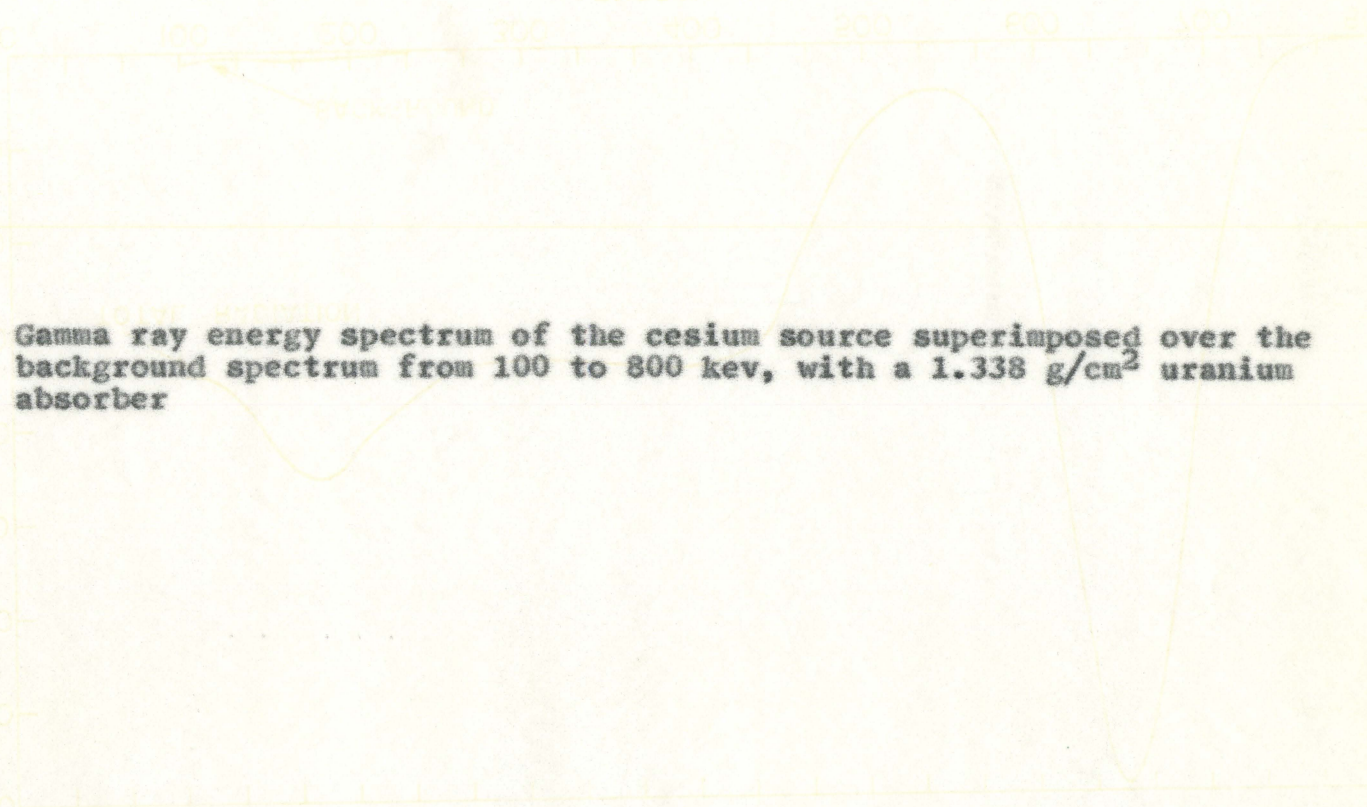

Figure 3. Gamma ray energy spectrum of the cesium source superimposed over the background spectrum from 100 to 800 kev, with a 1.338 g/cm^2 uranium absorber

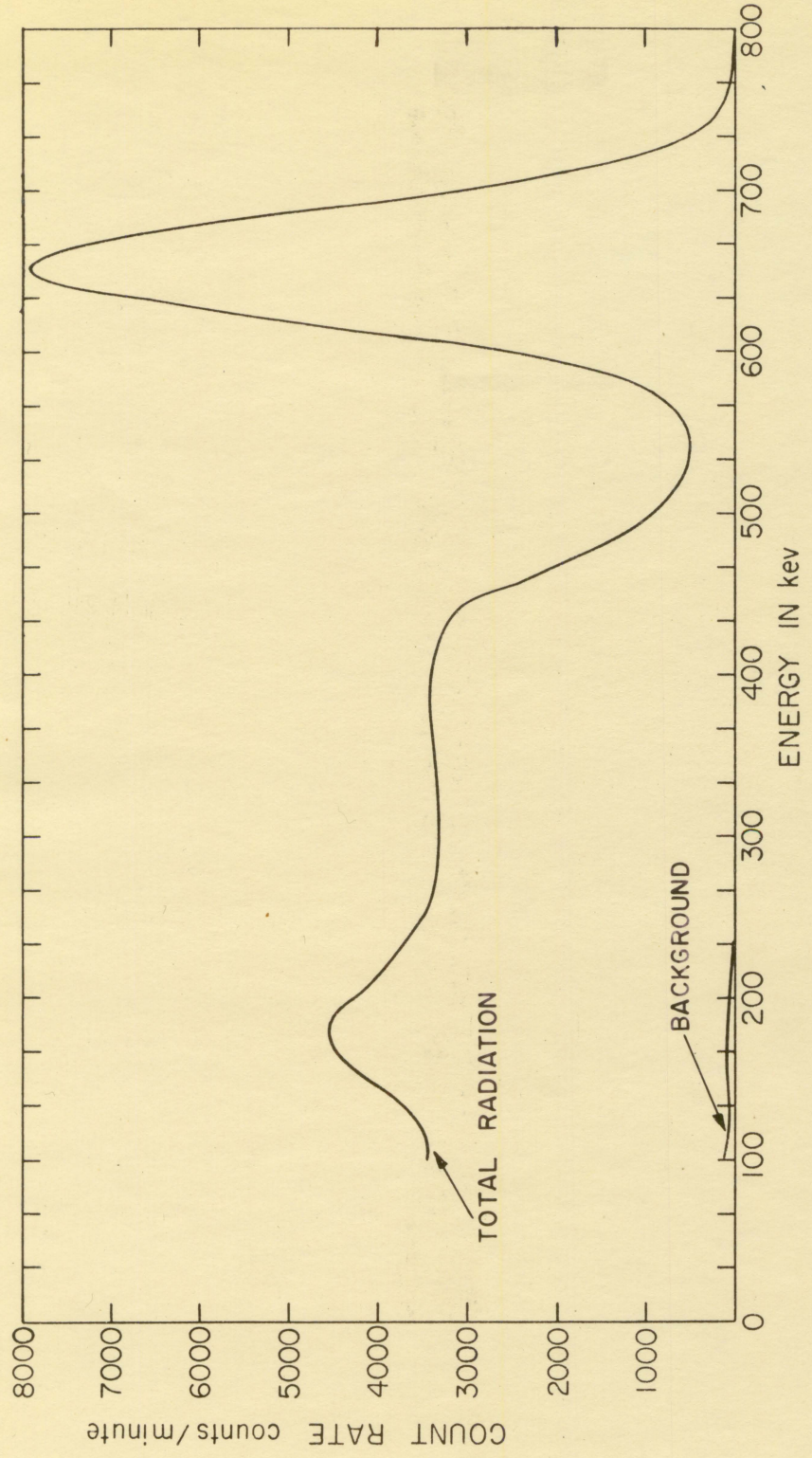
COUNT RATE counts/minute
8000
7000
6000
5000
4000
3000
2000
1000
0
100
200
300
400
500
600
700
800
ENERGY IN kev
TOTAL RADIATION
BACKGROUND

Figure 4. Gamma ray energy spectrum of the cesium source from 100 to 800 kev, with a 9.561 g/cm^2 uranium absorber

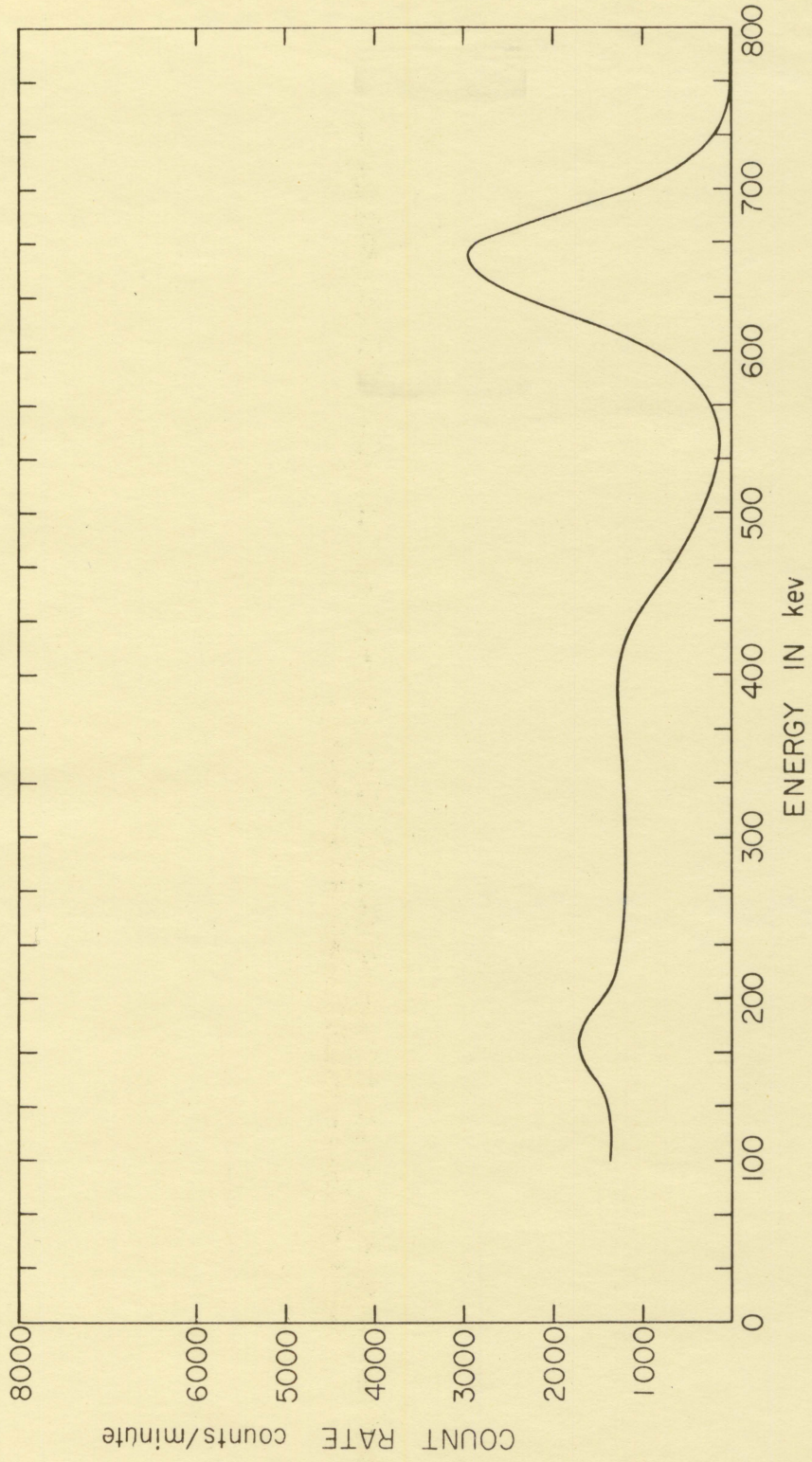
COUNT RATE counts/minute
8000
6000
5000
4000
3000
2000
1000
0
100
200
300
400
500
600
700
800
ENERGY IN kev

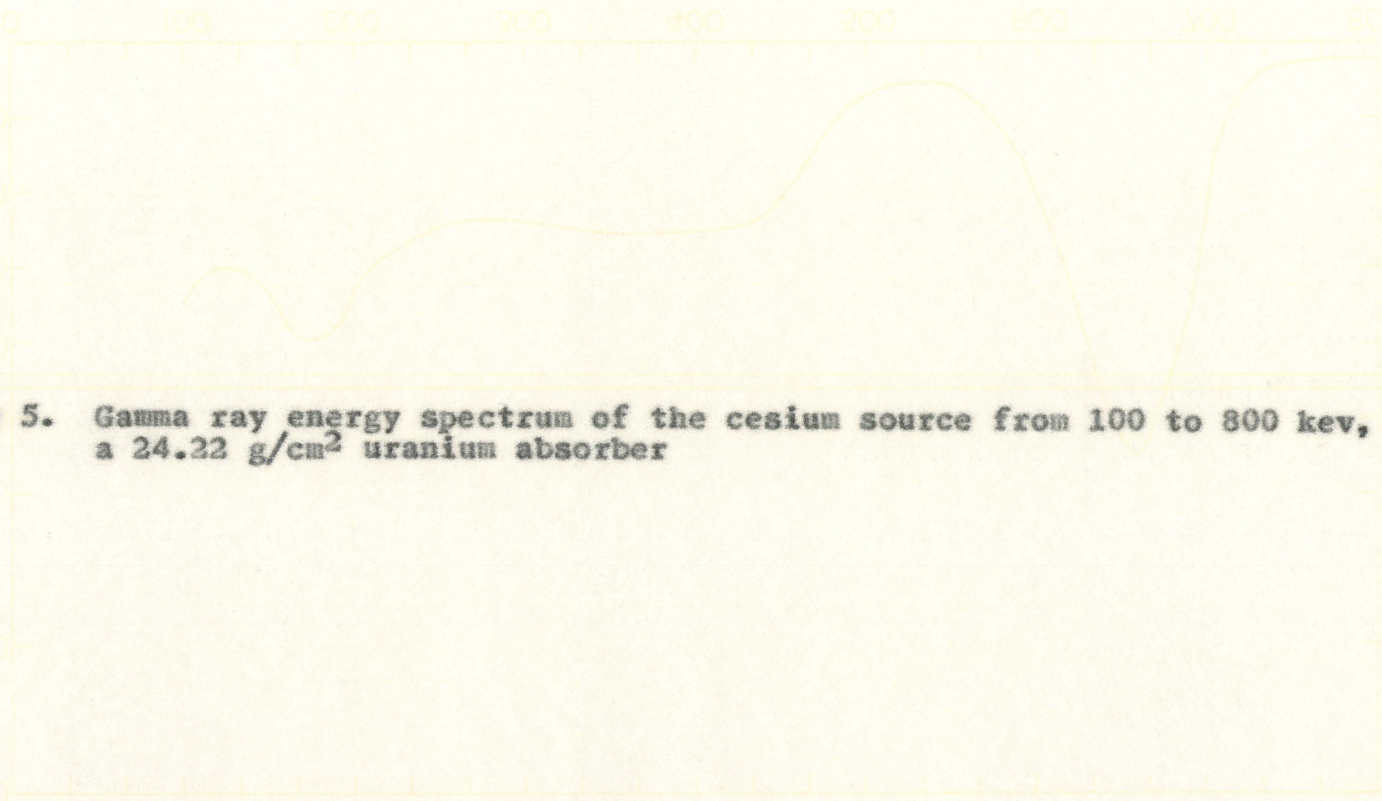

Figure 5. Gamma ray energy spectrum of the cesium source from 100 to 800 kev, with a 24.22 g/cm^2 uranium absorber

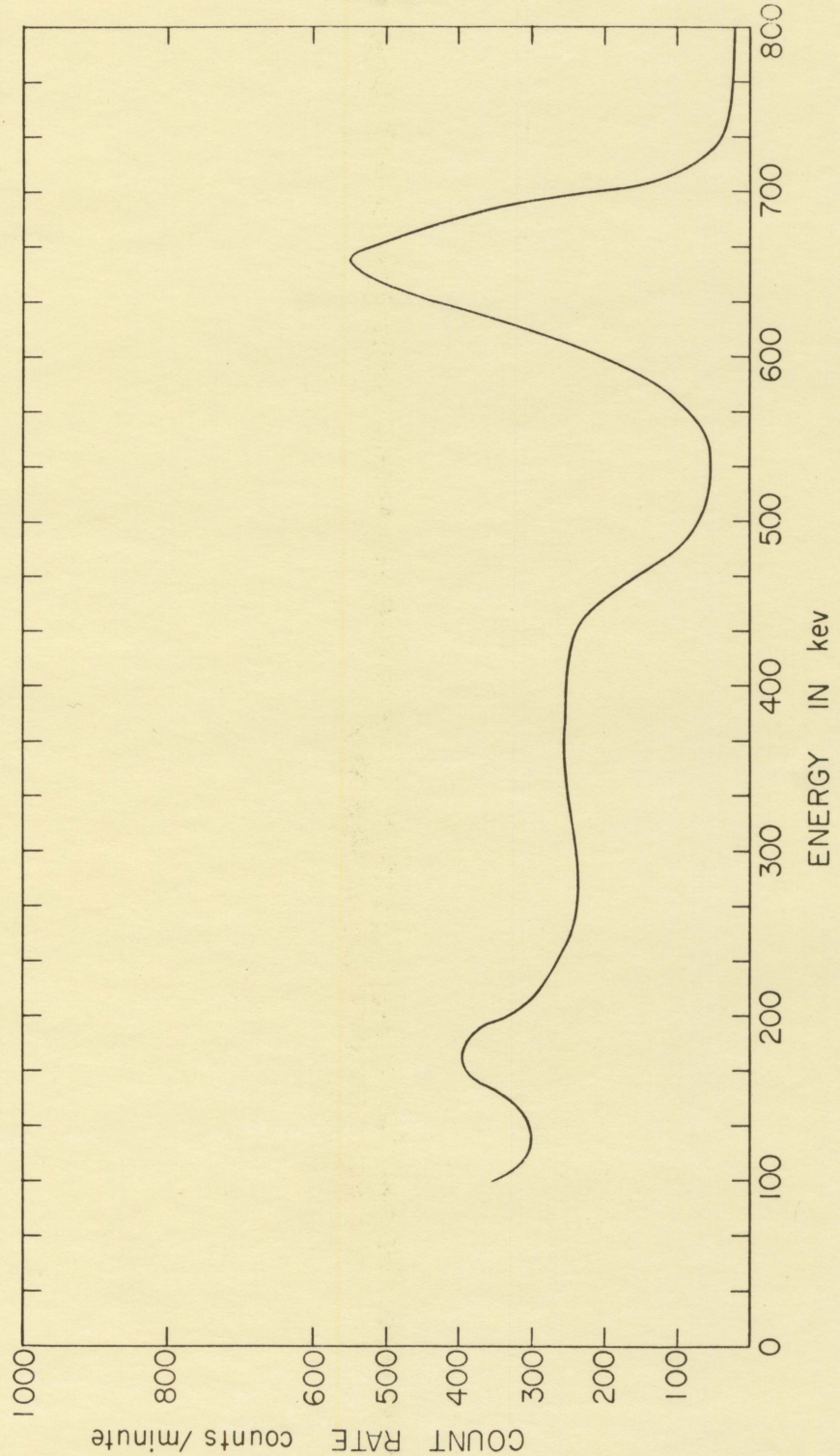
COUNT RATE counts /minute
1000
800
600
500
400
300
200
100
0
100
200
300
400
500
600
700
800
ENERGY IN kev

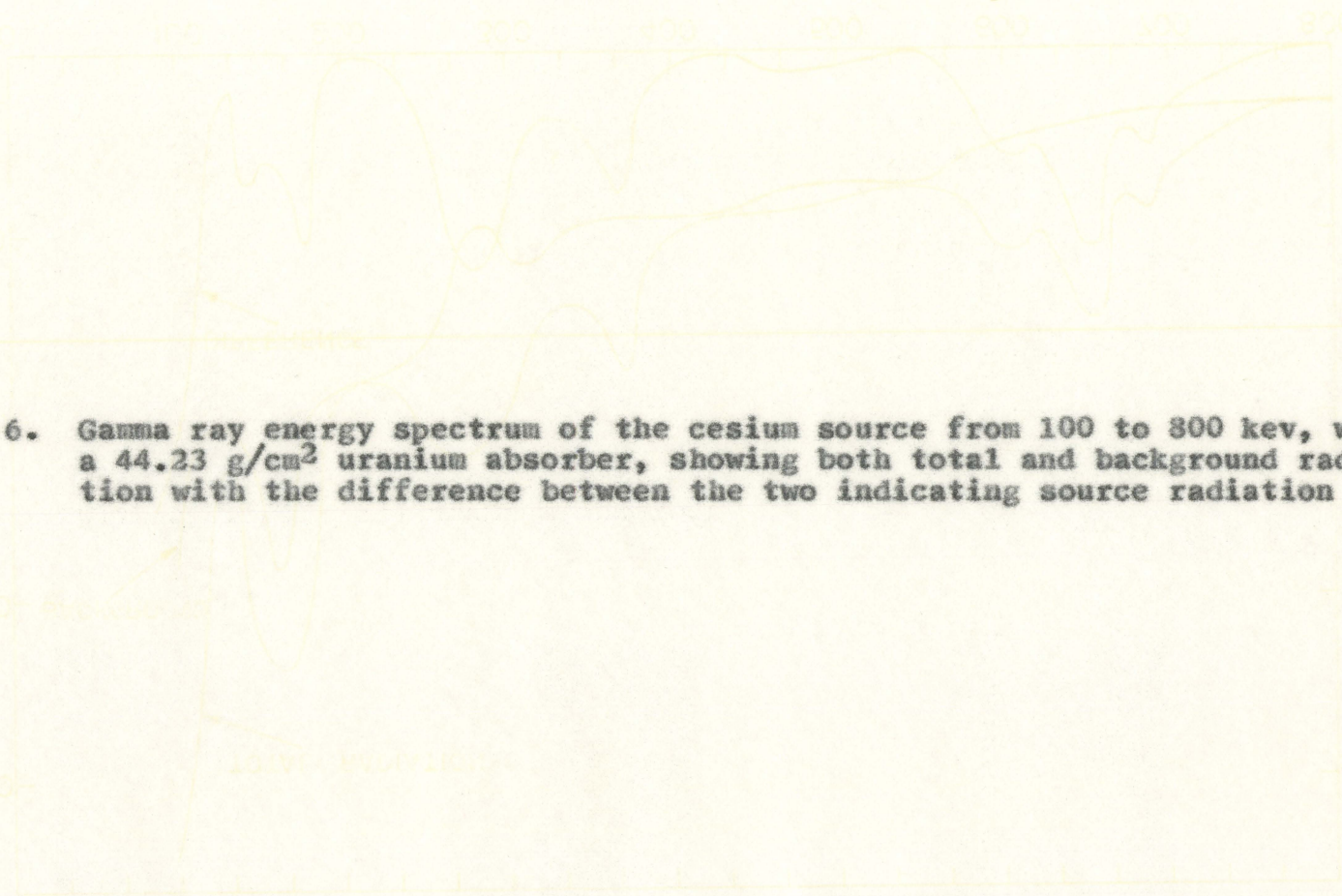

Figure 6. Gamma ray energy spectrum of the cesium source from 100 to 800 kev, with a 44.23 g/cm^2 uranium absorber, showing both total and background radiation with the difference between the two indicating source radiation

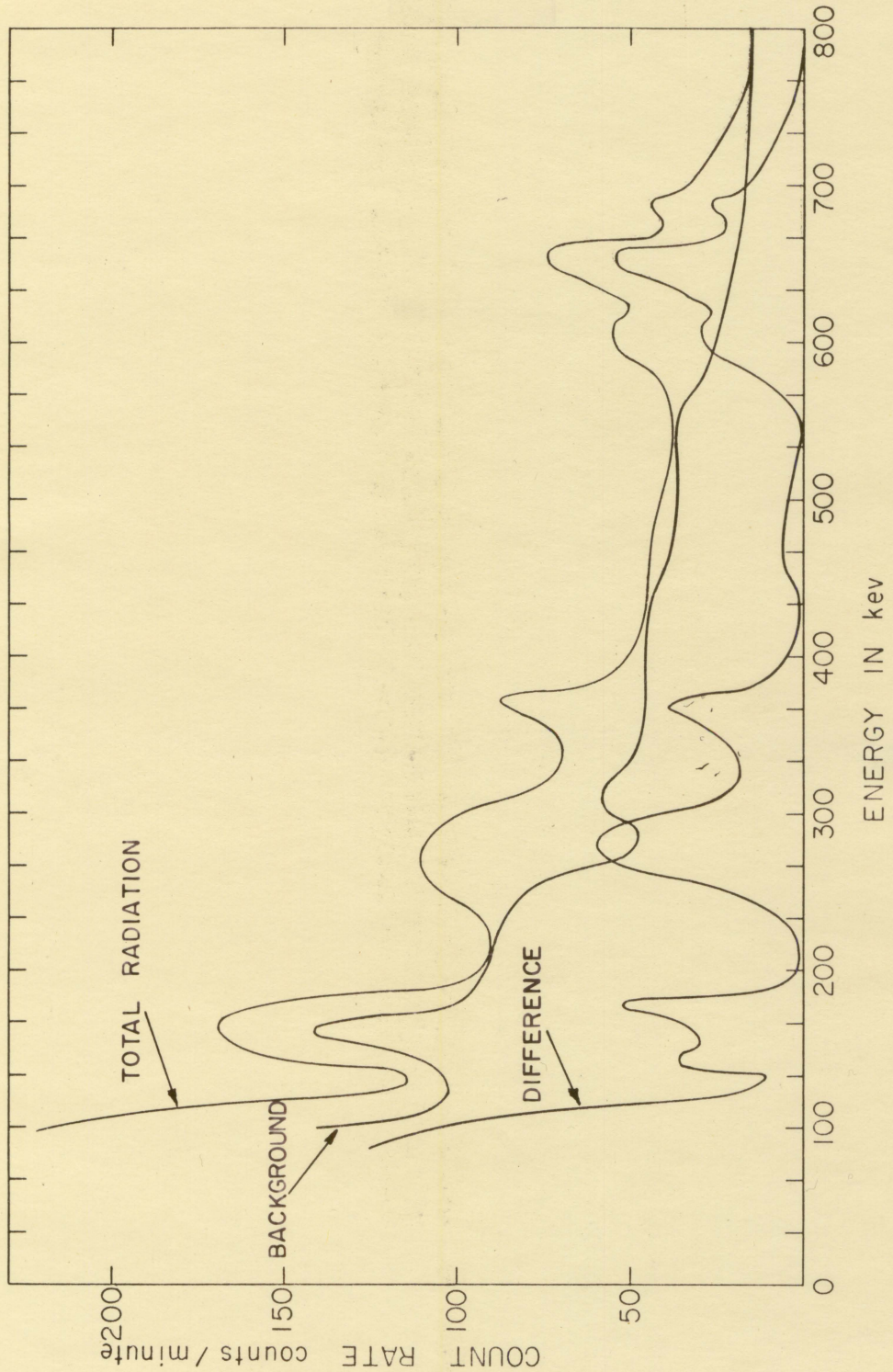
TOTAL RADIATION
BACKGROUND
DIFFERENCE
COUNT RATE counts / minute
200
150
100
50
0
100
200
300
400
500
600
700
800
ENERGY IN kev

the unabsorbed and unscattered radiation reaching the detector and the total background effect for that particular uranium absorber thickness of 44.23 gm/cm^2. This more accurately illustrates the relative contribution of the penetrating radiation.

The predominent peak on each of the spectrograms is at the expected value of 0.662 Mev. This of course corresponds to the energy of the primary emitted gamma ray. The peak itself is a measure of the number of unabsorbed and unscattered photons reaching the detector. The decrease in the peak with uranium absorbers in place is a measure of the number of photons which are both scattered and absorbed.

At lower energies, the effect of Compton scattering becomes apparent. This internal Compton scattering is due to two processes. The first process is the interaction of the gamma rays with the scintillation crystal. When a photon is scattered in a collision with an electron in the crystal, the scattered photon may either be absorbed in the crystal or pass on through the crystal. If it is absorbed, the detector will register the complete interaction as a single pulse with the height equal to the energy of the incident photon. But if the scattered photon passes through the crystal, the detector will register a pulse with a height equal to the energy lost

by the incident photon in the collision. As high energy photons have a greater tendency to penetrate the crystal without being absorbed, the effect will be more pronounced for collisions at small angles. These low angle collisions result in little energy loss to the photons. Thus a greater amount of this type of Compton scattering will be registered in the lower energy range.

The other Compton scattering process present is due to the liner of the detector. A portion of the photons incident in the scintillation crystal will penetrate it with no interaction. Part of these will be scattered back into the crystal by the liner. The scattering angle would have to be at least 90° for the photon to return to the crystal. Thus this effect of internal scattering should begin to appear at an energy corresponding to a scattering angle of 90° and then hold fairly constant throughout the lower energies. This energy is calculated to be 435 kev. Examination of the spectrograms indicates good correlation here as the curve rises at about 435 kev and then maintains at least that plateau level throughout.

Further down the energy scale other effects are added to the Compton scattering. These effects appear as peaks on top of the scattering plateau on the spectrograms.

On all spectrograms recorded in this experiment, a second major peak was present in the vicinity of 184 to 200 kev.

This peak decreased with increased absorber thickness with a half-thickness essentially identical to that of the 662 kev peak. This phenomena and the probable explanation are discussed in the following section.

This second major peak is the final contribution shown on the spectrograms. However just below the cut-off point of 100 kev on the spectrogram lies the characteristic K X-ray from photoelectric absorption in uranium. The energy of this X-ray is equal to the energy difference between the K and L shells and has a value of 92 kev. The effect of this X-ray can just begin to be seen on the spectrograms as an increasing slope is noted on all figures at 100 kev.

B. Interpretation of Data

There were two methods used in calculating the variation of gamma ray flux with absorber thickness. The first method involves energy flux or intensity and the second deals with number flux.

If I(E) is the intensity of gamma radiation of a particular energy and is defined by $I(E) = EN(E)$, then the variation in I(E) with increasing absorber thickness can be determined by measuring the area under the spectrogram curves for that particular energy. The areas under the 662 kev peak have been compiled and are presented in Table 3. These areas are ex-

pressed in counts as the abscissa, energy, is easily converted to time since 100 kev required a three minute spectrometer run. Also shown in Table 3 is the total area under the entire spectrogram curve. This of course gives a measure of the total intensity penetrating the absorber.

Table 3. Variation of areas with absorber thicknesses

Absorber thickness (g/cm^2)	Area under 662 kev peak net counts	Area under entire curve net counts
1.338	10018	198783
4.887	7745	124060
9.561	4252	81278
14.597	2459	48440
24.22	854	16352
33.85	283	5516
40.42	133	2403
44.23	82	1756

These values are plotted on semi-logarithmic plots and shown in Figures 7 and 8. The resulting curves were straight lines and a graphical illustration of $I(E) = I_o(E)e^{-\mu x}$.

The number flux method is based on the fact that if N(E) is the number of gamma rays of a particular energy, then the variation in N(E) with increasing absorber thickness can be

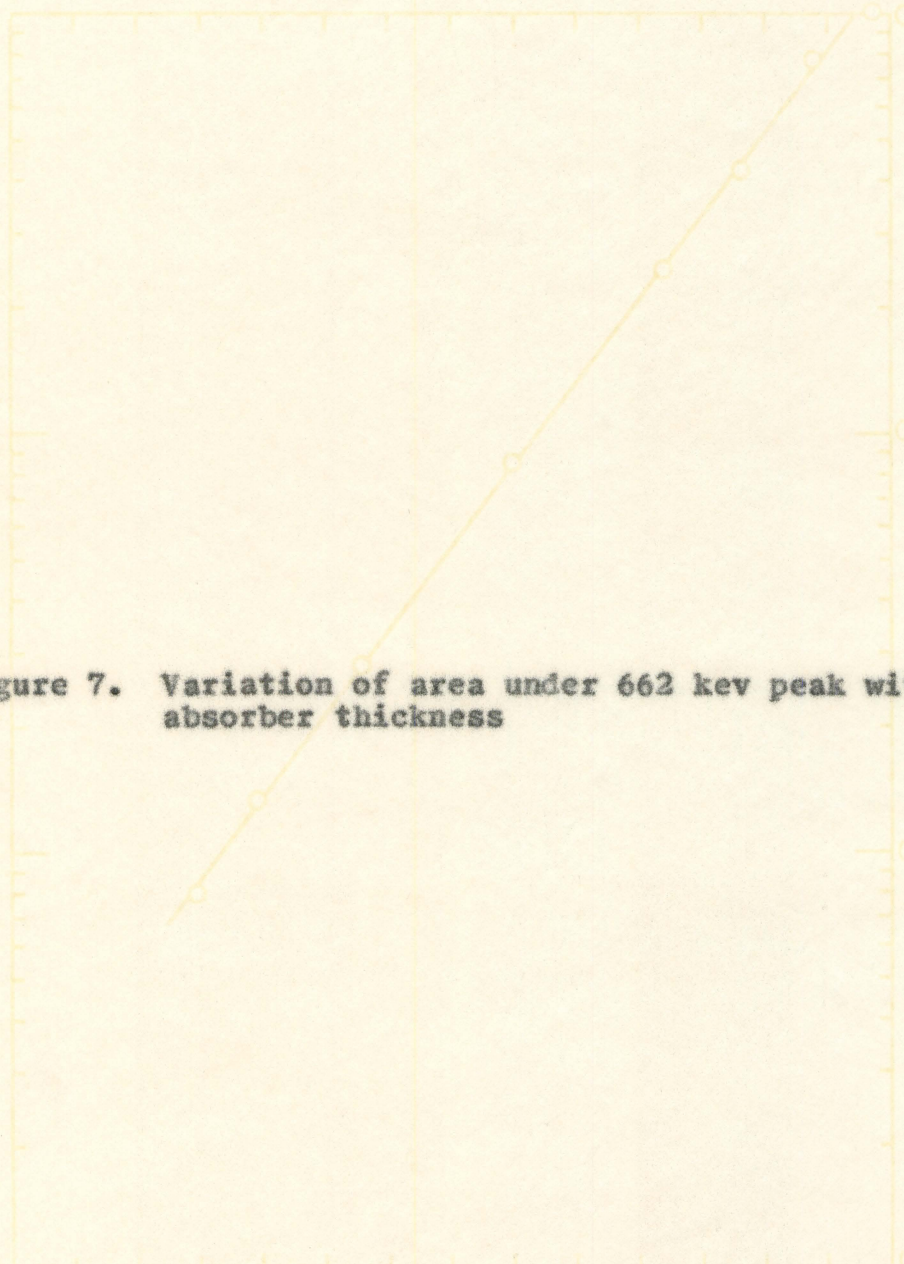

Figure 7. Variation of area under 662 kev peak with absorber thickness

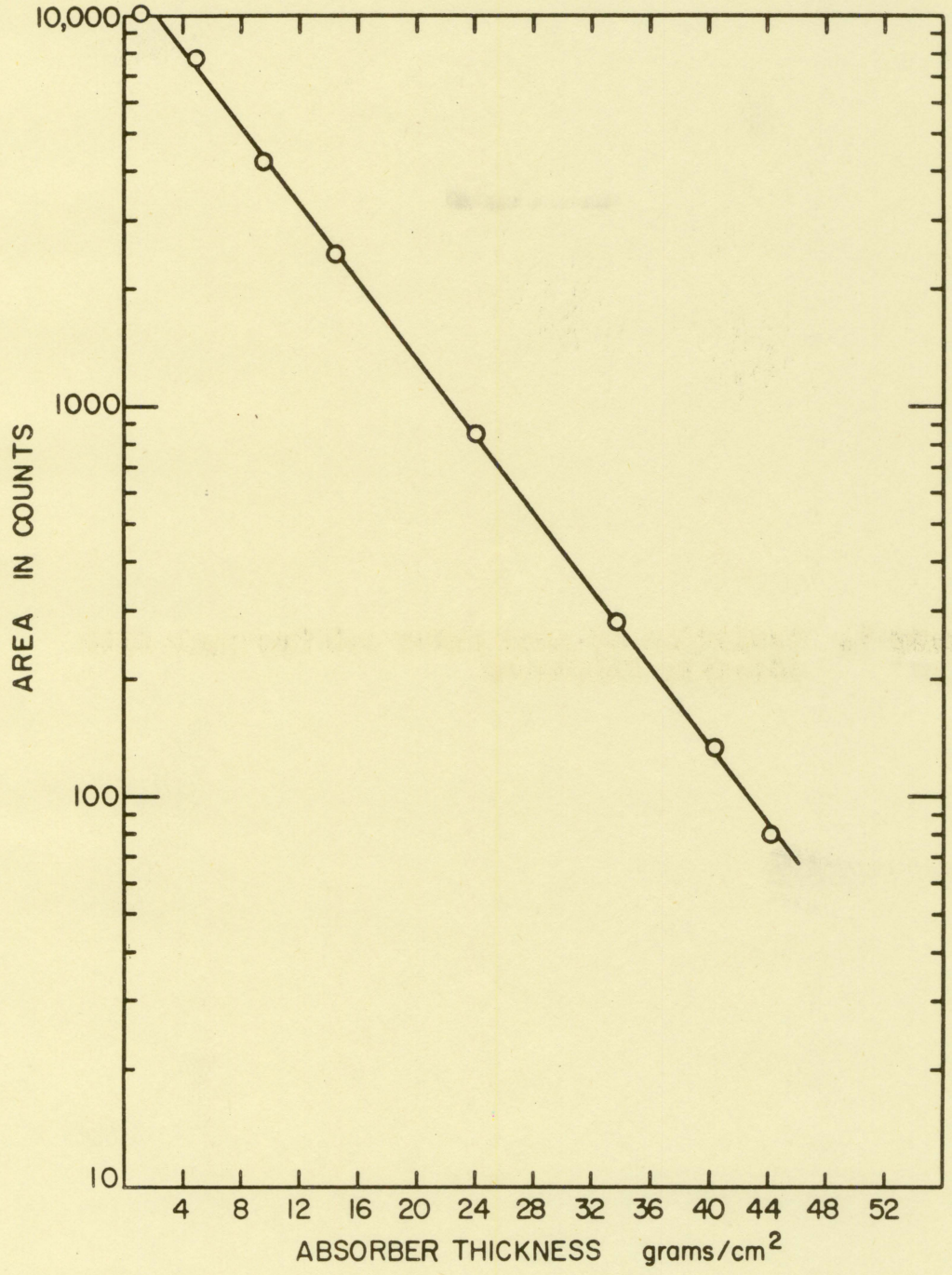
10,000
1000
100
10
AREA IN COUNTS
4
8
12
16
20
24
28
32
36
40
44
48
52
ABSORBER THICKNESS grams/cm2

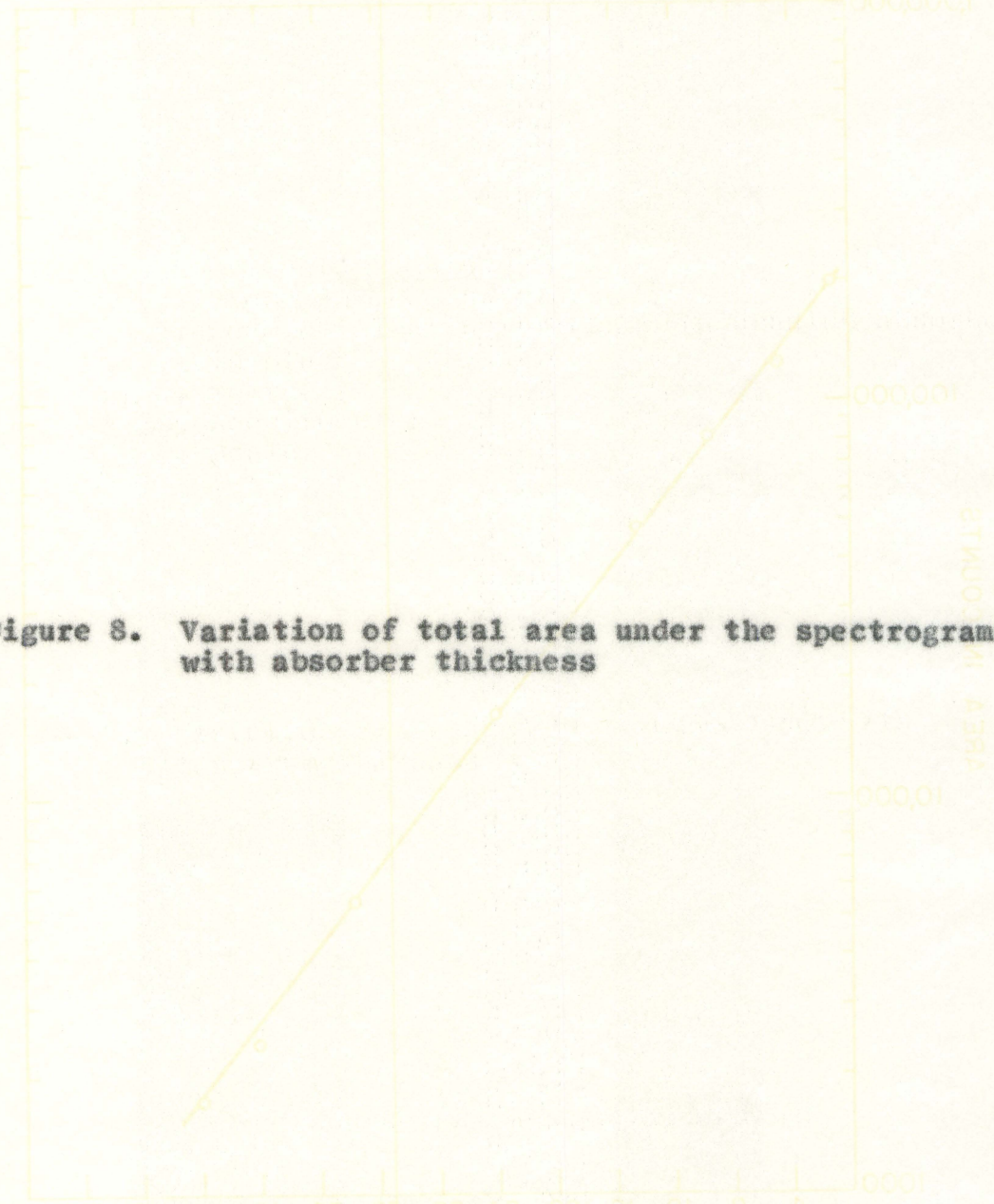

Figure 8. Variation of total area under the spectrograms with absorber thickness

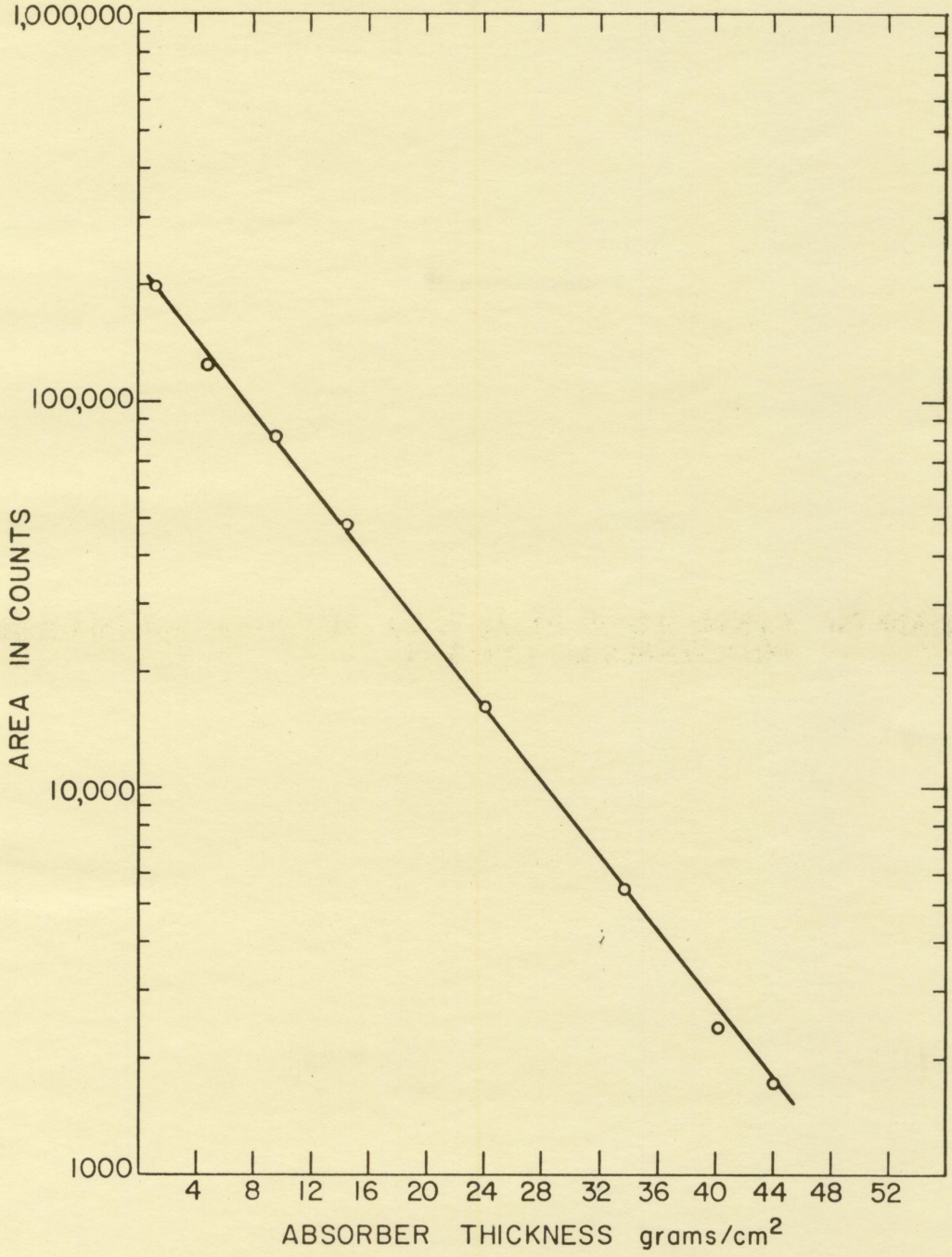
1,000,000
100,000
10,000
1000
AREA IN COUNTS
4
8
12
16
20
24
28
32
36
40
44
48
52
ABSORBER THICKNESS grams/cm2

determined by measuring the count rate at a particular energy point on each of the spectrograms. These measurements have been made on all the spectrograms including the corresponding background spectrograms. The data have been compiled in Table 4 showing values of the count rate versus absorber thickness at both 662 kev and 184 kev.

Table 4. Variation of count rate with absorber thickness and energy

Absorber thickness (g/cm^2)	Counts per minute	
	184 kev	662 kev
1.338	4480	7905
4.887	2810	5090
9.561	1620	2940
14.597	940	1600
24.22	310	530
33.85	100	173
40.42	48	88
44.23	30	54

These values are plotted on a semi-logarithmic plot and shown in Figure 9. The straight lines of the resulting curves indicate exponential variation of count rate with absorber thickness and correlation with $N(E) = N_o(E)_e^{-\mu x}$.

Attention is called to the fact that the slopes of these

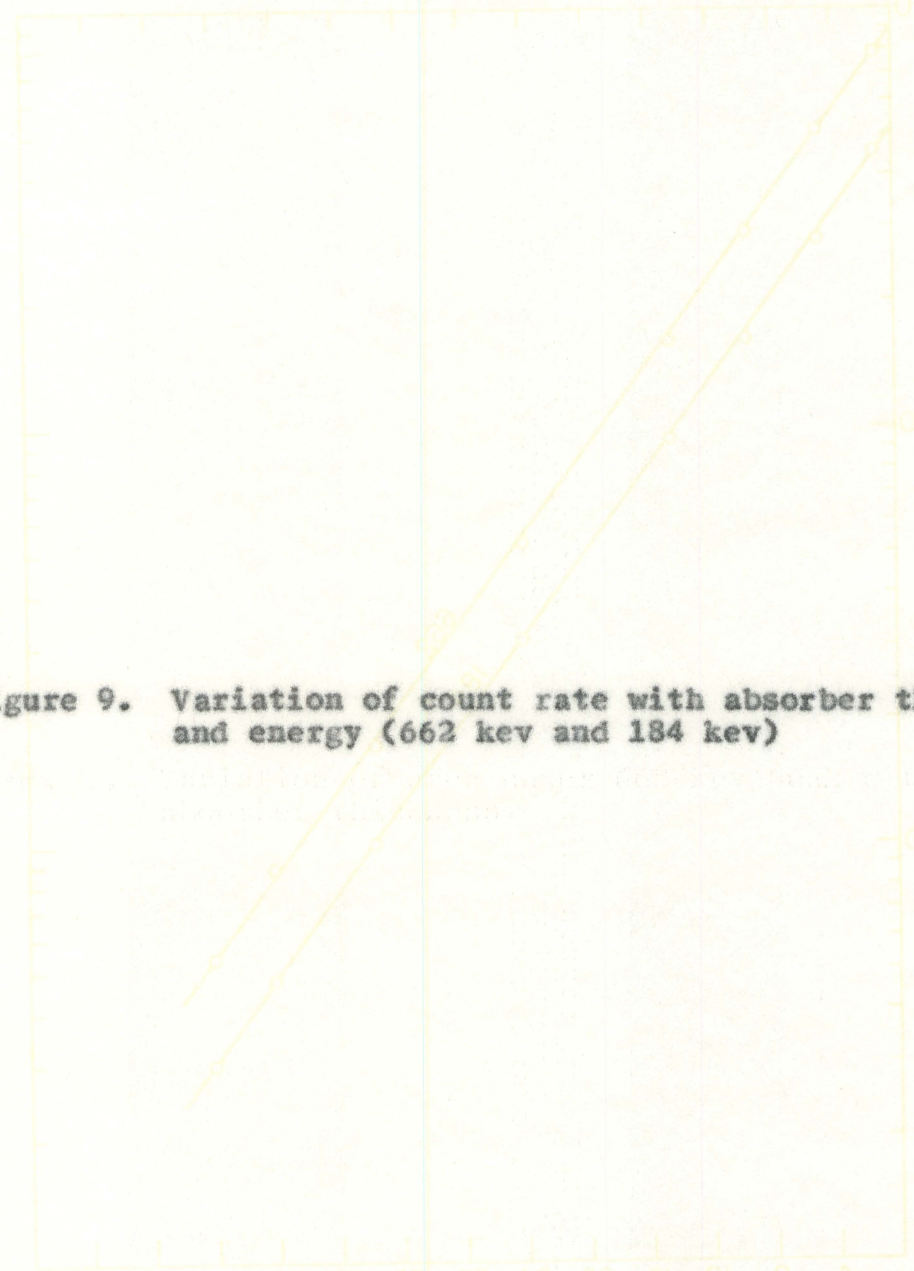

Figure 9. Variation of count rate with absorber thickness and energy (662 kev and 184 kev)

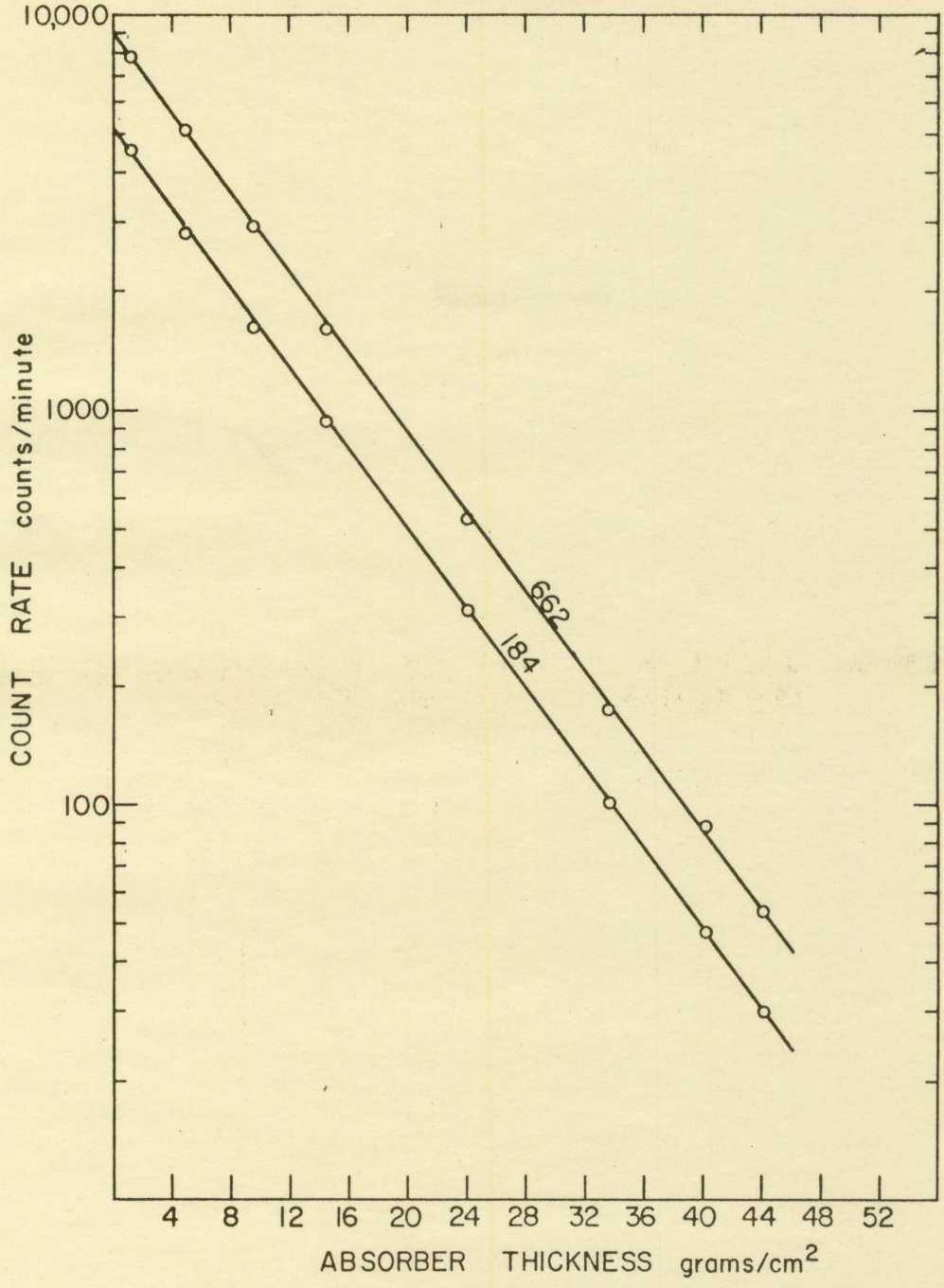
10,000
1000
100
COUNT RATE counts/minute
662
184
4
8
12
16
20
24
28
32
36
40
44
48
52
ABSORBER THICKNESS grams/cm2

two lines are practically identical. This is rather good evidence that the contributing photons are of the same energy. The most probable explanation is that after the 662 kev photons penetrated the uranium absorber, they were scattered in the lead surrounding the scintillation crystal. As the probe was within a lead container and placed next to a lead brick, ample scattering opportunity was offered these photons. This scattering process might be expected to result in a broader peak than that observed. To explain the relative sharpness of this peak it is postulated that scattering at approximately 180° is more probable than at smaller angles, due to the particular geometrical placement of the detector and lead shielding. Compton scattering of 662 kev gamma rays at 180° would give a secondary gamma ray of 184 kev by calculation using Equation 2.

C. Mass Absorption Coefficients

The quantity most conveniently obtained from an absorption curve for gamma radiation is the half-thickness. This is the thickness of absorber required to reduce the gamma ray intensity to one half the initial value. Thus if the half-thickness d is defined as that value of x which makes $Id = \frac{1}{2} I_o$, then $d = \frac{0.693}{\mu}$. Values of the half-thickness were determined from the three curves in Figures 7, 8, and 9. These values are shown in Table 4a. The two curves in Figure 9 have the same slope and hence result in an identical value of the

absorber thickness required to reduce the gamma ray intensity by one half. Knowing the half-thickness, the mass absorption coefficient follows immediately. The corresponding values of the mass absorption coefficient are also listed in Table 4a.

Table 4a. Gamma ray mass absorption coefficients and half-thickness values

Type of data	Half thickness	Mass absorption coefficient
662 kev peak rate	6.0	0.115
184 kev peak rate	6.0	0.115
662 kev peak area	6.1	0.114
Entire curve area	6.3	0.110

Since the two values corresponding to the 662 kev curves are practically identical, the value of $\mu(E)$ can thus be said to be practically the same for the variation in both N(E) and I(E).

G. R. White (13) has compiled extensive data on the subject of electromagnetic radiation and has several tables showing values considered quite accurate for gamma ray mass absorption coefficients. Table 5 lists these values of μ for uranium.

These values of μ for uranium published by White were

plotted on a logarithmic graph in Figure 10. The experimentally determined value of μ is 0.114. This is the value resulting from the consideration of I(E) and is taken from the curve representing the area under the 662 kev peak. This value is plotted on the graph to compare it with the published values. As is illustrated in Figure 10, the experimental value fell exactly on the curve of theoretical values.

Table 5. Gamma ray mass absorption coefficient, μ, for uranium in cm^2/g (after G. R. White)

Energy mev	$\frac{\mu}{cm^2/g}$
0.05	7.16
0.06	4.28
0.08	1.93
0.10	1.06
0.1163 K edge	0.715
0.1163 K edge	4.64
0.15	2.42
0.20	1.17
0.30	0.452
0.40	0.259
0.50	0.176
0.60	0.136
0.80	0.0952
1.00	0.0757

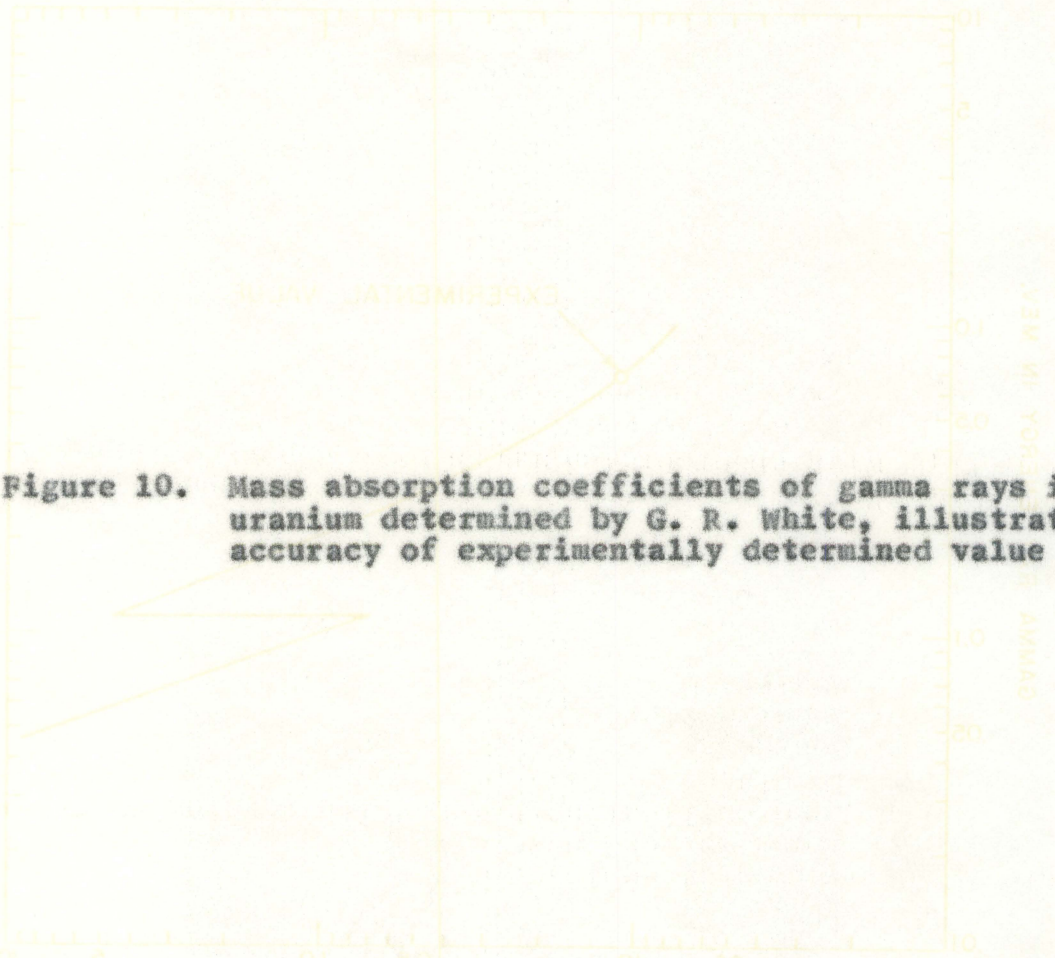

Figure 10. Mass absorption coefficients of gamma rays in uranium determined by G. R. White, illustrating accuracy of experimentally determined value

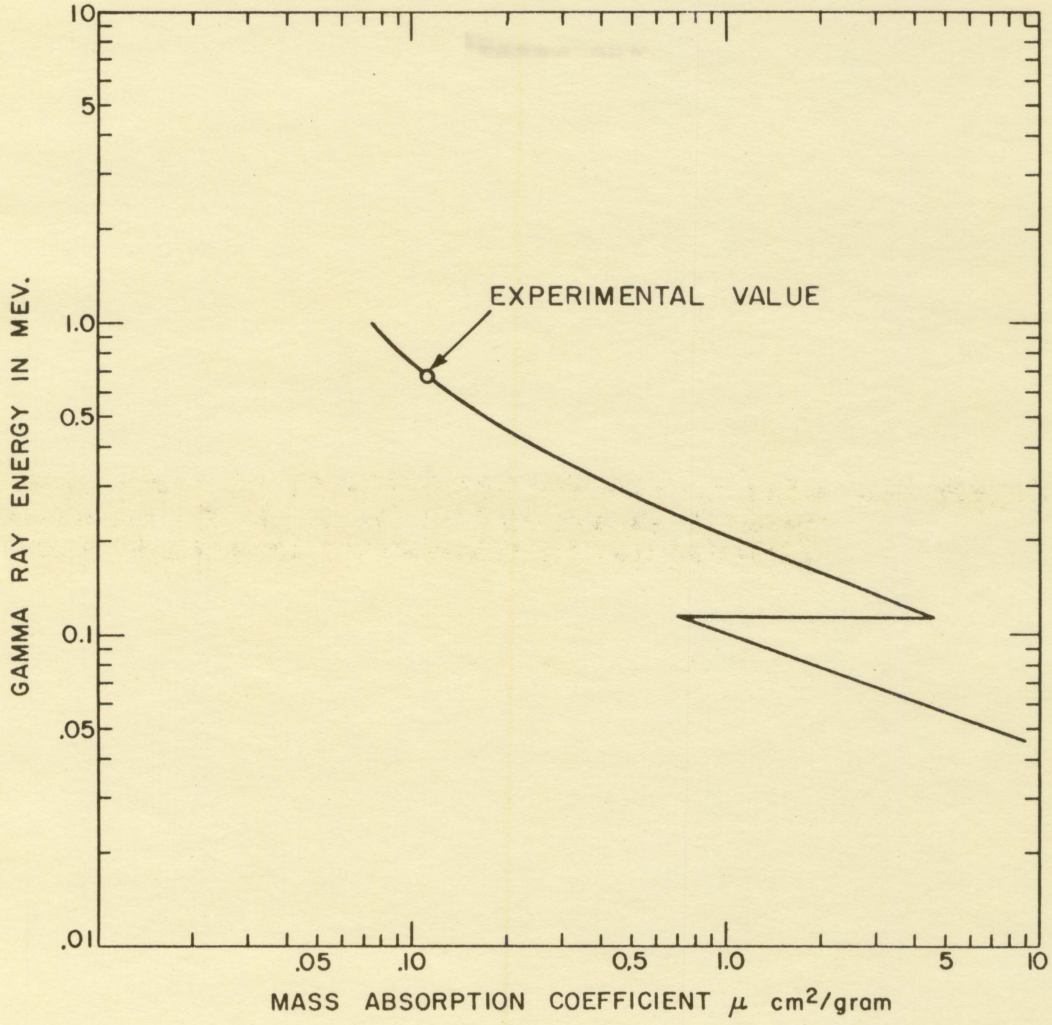
10
5
1.0
0.5
0.1
.05
.01
GAMMA RAY ENERGY IN MEV.
EXPERIMENTAL VALUE
.05
.10
0.5
1.0
5
10
MASS ABSORPTION COEFFICIENT μ cm²/gram

VI. CONCLUSIONS

The value of the mass absorption coefficient obtained by this experiment was quite accurate indicating excellent agreement with theory.

The scintillation detector and the scintillation spectrometer are again proven reliable in calculating gamma ray attenuation. Although previously proven successful in other attenuation studies, the use of the heavy material uranium, radioactive in itself, as the absorber, is unique and clearly illustrates the effectiveness of the scintillation spectrometer method in the gamma radiation field.

VII. LITERATURE CITED

1. Bethe, H. A. and Ashkin, J. Penetration of gamma rays. In Segre, E., ed. Experimental nuclear physics. Vol. 1. pp. 305-349. New York, N. Y., John Wiley and Sons, Inc. 1953.

2. Davisson, C. M. and Evans, R. D. Gamma ray absorption coefficients. Rev. Mod. Phys. 24:79-107. 1952.

3. Fano, U. Gamma ray attenuation. Nucleonics 11, No. 8: 8-12; and No. 9:55-61. 1953.

4. Friedlander, G. and Kennedy, J. W. Nuclear and radiochemistry. New York, N. Y., John Wiley and Sons, Inc. 1955.

5. Goldstein, H. The attenuation of gamma rays and neutrons in reactor shields. Washington, D.C., U.S.Govt. Print. Off. 1957.

6. _____ and Wilkins, J. E., Jr. Calculations of the penetrations of gamma rays. U.S.Atomic Energy Commission Report NYO-3075 [New York Operations Office, AEC]. June 30, 1954.

7. Heitler, W. Quantum theory of radiation. 3rd ed. New York, N. Y., Oxford University Press. 1954.

8. Kaplan, I. Nuclear physics. Cambridge, Mass., Addison-Wesley Publishing Company, Inc. 1955.

9. Latter, R. and Kahn, H. Gamma ray absorption coefficients. Rand Corp. R-170. 1949.

10. Nelms, A. T. Graphs of the Compton energy angle relationship and the Klein Nishina formula from 10 kev to 500 Mev. Nat. Bur. Standards Circular 542. 1953.

11. Segre, E. Experimental nuclear physics. Vol. 1. New York, N. Y., John Wiley and Sons, Inc. 1953.

12. Snyder, W. S. and Powell, J. L. Absorption of gamma rays. U.S.Atomic Energy Commission Report ORNL-421 [Oak Ridge National Laboratory]. March 14, 1950.

13. White, G. R. Gamma ray attenuation coefficients from 10 kev to 100 Mev. Nat. Bur. Standards Circular 583. 1957.

VIII. ACKNOWLEDGMENTS

I would like to express my sincere gratitude to Professor A. F. Voigt for his helpful advise and timely counsel throughout this investigation.

Thanks also are due to Mr. Melvin Foster for his encouragement and assistance during the course of this investigation and to my wife, Nancy, for her patience and understanding.

Finally I would like to express my appreciation to the United States Air Force and the Air Force Institute of Technology for the opportunity of receiving this education.

IX. APPENDIX A. TABULATION OF DATA

Table 6. Tabulation of data

Absorber thickness g/cm^2	.662 Mev peak rate	Background	.662 Mev peak net rate	Area under .662 Mev peak	Background area	Net area under .662 Mev peak	184 kev peak	Background	184 kev peak net rate	Area under entire curve	Background area	Net total area
1.338	7920	15	7905	10024	6	10018	4560	80	4480	201600	2817	198783
4.887	5110	20	5090	7760	15	7745	2900	90	2810	127967	3907	124060
9.561	2960	20	2940	4267	15	4252	1720	100	1620	86117	4837	81278
14.597	1615	15	1600	2480	21	2459	1040	100	940	53655	5212	48440
24.22	555	25	530	884	30	854	410	100	310	22431	6079	16352
33.85	198	25	173	311	28	283	220	120	100	11881	6365	5516
40.42	113	25	88	163	30	133	168	120	48	9000	6597	2403
44.23	75	21	54	102	20	82	172	142	30	8045	6289	1756